

# Calcineurin homologous proteins regulate the membrane localization and activity of sodium/proton exchangers in *C. elegans*

Erik Allman,<sup>1,3</sup> Qian Wang,<sup>1</sup> Rachel L. Walker,<sup>1</sup> Molly Austen,<sup>1</sup> Maureen A. Peters,<sup>2</sup> and Keith Nehrke<sup>1</sup>

<sup>1</sup>Departments of Pharmacology and Physiology and Medicine, University of Rochester School of Medicine and Dentistry, Rochester, New York; <sup>2</sup>The Department of Biology, Oberlin College, Oberlin, Ohio; and <sup>3</sup>Department of Biochemistry and Molecular Biology, Pennsylvania State University, University Park, Pennsylvania

Submitted 1 October 2015; accepted in final form 9 November 2015

**Allman E, Wang Q, Walker RL, Austen M, Peters MA, Nehrke K.** Calcineurin homologous proteins regulate the membrane localization and activity of sodium/proton exchangers in *C. elegans*. *Am J Physiol Cell Physiol* 310: C233–C242, 2016. First published November 11, 2015; doi:10.1152/ajpcell.00291.2015.—Calcineurin B homologous proteins (CHP) are *N*-myristoylated, EF-hand Ca<sup>2+</sup>-binding proteins that bind to and regulate Na<sup>+</sup>/H<sup>+</sup> exchangers, which occurs through a variety of mechanisms whose relative significance is incompletely understood. Like mammals, *Caenorhabditis elegans* has three CHP paralogs, but unlike mammals, worms can survive CHP loss-of-function. However, mutants for the CHP ortholog PBO-1 are unfit, and PBO-1 has been shown to be required for proton signaling by the basolateral Na<sup>+</sup>/H<sup>+</sup> exchanger NHX-7 and for proton-coupled intestinal nutrient uptake by the apical Na<sup>+</sup>/H<sup>+</sup> exchanger NHX-2. Here, we have used this genetic model organism to interrogate PBO-1's mechanism of action. Using fluorescent tags to monitor Na<sup>+</sup>/H<sup>+</sup> exchanger trafficking and localization, we found that loss of either PBO-1 binding or activity caused NHX-7 to accumulate in late endosomes/lysosomes. In contrast, NHX-2 was stabilized at the apical membrane by a nonfunctional PBO-1 protein and was only internalized following its complete loss. Additionally, two *pbo-1* paralogs were identified, and their expression patterns were analyzed. One of these contributed to the function of the excretory cell, which acts like a kidney in worms, establishing an alternative model for testing the role of this protein in membrane transporter trafficking and regulation. These results lead us to conclude that the role of CHP in Na<sup>+</sup>/H<sup>+</sup> exchanger regulation differs between apical and basolateral transporters. This further emphasizes the importance of proper targeting of Na<sup>+</sup>/H<sup>+</sup> exchangers and the critical role of CHP family proteins in this process.

transporter; trafficking; sodium/proton exchange

CALCINEURIN B HOMOLOGOUS PROTEIN (CHP) belongs to the EF-hand calcium-binding family and has been shown to regulate vesicle trafficking, cell proliferation, gene transcription, and Na<sup>+</sup>/H<sup>+</sup> exchanger (NHE) activity (23, 24, 26, 29, 36, 43). There are three CHP paralogs in mammals. CHP1 is broadly expressed and was first identified by several groups working in parallel: first, through its binding to the cytoplasmic COOH-terminal tail of the ubiquitous mammalian NHE1 (21, 28) and second, through a role in protein trafficking (8). CHP family proteins have since been suggested to be required for both basal and calcium-stimulated NHE activity, NHE biosynthetic maturation, transport to the membrane, and stabilization of the transporter once it is there (16, 28, 33, 43, 53, 54). CHP1's affinity for calcium increases greatly when it is bound to

NHE1, suggesting a possible connection between calcium signaling and stimulation of NHE activity (42). However, given the large number of outputs credited to CHP1, it has been difficult to ascertain what effects can be attributed to discrete functional modalities. In addition, potential CHP-binding sites are likely conserved among NHEs, including organelle transporters (55), and, in some cases, CHP1 has been shown to regulate the activity of other NHEs such as NHE3 (16, 20, 31). Further complexity arises from two additional CHP paralogs, CHP2 (4, 35, 37, 44) and CHP3 (22, 27, 32, 45), which are less well characterized but have nonetheless been shown to interact with NHEs and regulate their activity.

Developing a more nuanced understanding of CHP function in a complex systems environment has been complicated by the fact that genetic ablations are apparently lethal in mammals. However, a point mutant in CHP1 was recently identified in the vacillator mutant mouse and demonstrated quite elegantly to cause degeneration of Purkinje cell axons (30). The authors suggested that neuronal CHP1 is necessary for targeting of NHE1 and that effective axonal pH homeostasis supports axonal health.

We also recently showed that loss-of-function (*lf*) mutations in the *Caenorhabditis elegans* CHP family member *pbo-1* are tolerated (51). *Pbo-1* is largely expressed in the nematode intestine, and *pbo-1* mutants phenocopy the loss of intestinal NHEs, suggesting an evolutionarily conserved role in regulating their function (51). In brief, there are two particular NHEs in the nematode intestine, NHX-2 and NHX-7, that have been shown to contribute to intestinal homeostasis and whose loss elicits overt phenotypes (38).

NHX-2 is an apical membrane transporter whose expression is restricted to the intestine and whose function has been linked to that of the proton-dipeptide symporter OPT-2 (39, 40). NHX-2 is closely related to mammalian NHE3, which is also found at the apical membrane of intestinal epithelia and acts in a similar capacity (48, 49). Mutants in NHX-2 exhibit cytoplasmic acidosis, reduced dipeptide absorption, and a starvation phenotype, and RNA interference (RNAi) has been used as a genetic dietary restriction mimetic (39). NHX-7 (also called PBO-4) is a basolateral membrane transporter whose expression is restricted to the posteriormost cells of the intestine and whose activity transiently acidifies the extracellular space between the intestine and adjacent body wall muscle, causing those muscle cells to contract (9, 46). Proton extrusion is directed by intestinal oscillatory calcium signaling, which paces the rhythmic (~50-s period) defecation behavior in worms (15). Contraction of the posterior body wall muscles (pBoc) is the first and most visible step in the defecation motor

Address for reprint requests and other correspondence: K. Nehrke, Dept. of Medicine, Box 675, Univ. of Rochester Medical Center, 601 Elmwood Ave., Rochester, NY 14642 (e-mail: keith\_nehrke@urmc.rochester.edu).

program, and mutations in *nhx-7/pbo-4* reduce or eliminate pBoc without altering the underlying calcium signals.

Loss of PBO-1 in worms causes an amalgamation of these phenotypes, resulting in cellular acidosis, slow growth, reduced fat stores, and a weak pBoc muscle contraction without significantly altering oscillations in intestinal calcium (51). Moreover, mutation of a conserved CHP-binding domain in NHX-7 suppresses its ability to complement a *nhx-7/pbo-4* mutant, supporting the functional relevance of PBO-1 binding to impact NHX-7 activity (3). Coupled with the fact that rhythmic calcium oscillations occur in the intestinal cytoplasm every ~50 s and that CHP family proteins are thought to transduce calcium signals, these observations motivated us to further explore PBO-1's mechanism of action as related to NHE activity in the worm.

Our results support the idea that CHP family proteins stimulate trafficking, membrane retention, and activity of NHEs in a paralog-dependent manner and suggest that two new *pbo-1* paralogs may contribute to cell-specific functions through similar regulatory mechanisms. Together, these results represent one of the first reports of CHP loss-of-function, resulting in an NHE trafficking defect *in vivo*, and suggest a broadly conserved function between worm and mammalian systems.

## MATERIALS AND METHODS

**Strains, alleles, and culturing techniques.** Standard culture techniques were used to maintain nematodes on nematode growth medium (NGM)-agar plates seeded with OP50 bacteria (10). The wild-type strain is Bristol N2. Transgenes were introduced using microinjection with a *pha-1(+)* marker in a *pha-1(e2123ts)III* temperature-sensitive mutant strain, and transgenic progeny were selected for and maintained at 20°C. Genetic crosses were performed using standard mating techniques. *Pbo-1* mutant strains are TA105 *pbo-1(sa7)III* and TA111 *pbo-1(tm3716)III* as described previously (51). Strains containing the *pha-1(e2123ts)III* and calcineurin-like EF-hand protein family member (*chpf-2(ok2941)V*) alleles as well as the green fluorescent protein (GFP) integrated localization markers were obtained from the *C. elegans* Genetics Center (University of Minnesota), whom we kindly acknowledge, as well as the *C. elegans* Gene Knockout Consortium, and were outcrossed before use. A complete list of strains used in this work is shown in the Supplemental Material (Supplemental material for this article is available online at the journal website.).

**Molecular biology.** pELA3 and pKT107 are as previously described (3). An ~3-kb region of genomic DNA upstream of the start codon for the *chpf-2* gene was cloned into pFH6II::wCherry to generate pELA37. An ~2-kb region of genomic DNA upstream of the CEOP5248 operon and a small ~400-bp region of genomic DNA upstream of the start codon for the *chpf-1* gene was cloned into pFH6II::wCherry to generate pELA46 and pELA38, respectively.

**RNA interference.** Freshly transformed HT115 bacteria were grown at 37°C to midlog phase, induced with 1 mM isopropyl-β-D-thiogalactosidase for 1 h, and seeded on NGM plates. Larval L3 stage worms were placed on the RNAi plates and moved to new plates at 24 h, and their progeny were screened.

**Microscopy.** Images of transgenic strains and immunohistochemically stained animals were acquired at the University of Rochester Confocal Core. Images were acquired at room temperature using an Olympus IX81 inverted laser-scanning confocal microscope, with ×10 [numeric aperture (NA 0.40)], ×20 oil (NA 0.85), ×40 oil (NA 1.30), ×60 oil (NA 1.42), or ×100 oil (NA 1.40) objectives. Live worms were anesthetized with a solution of 1 mg/ml tetramisole in M9 buffer on 2% agarose pads under a cover slip. Z stacks ranging from 5 to 30 slices were obtained using the optimal slice depth. Olympus FluoView1000 software was used for image acquisition and

for post hoc image processing and analysis. The same acquisition parameters were used when analyzing relative transporter membrane abundance in separate genetic backgrounds.

**Osmotic stress assays.** To assess the excretory cell's ability to function following hypotonic exposure, worms were grown on NGM agar plates containing 500 mM NaCl for 24 h and after adaptation were moved back to a low-salt NGM plate. Subsequent survival was assayed after 12 h.

**Generation of the anti-NHX-2 antibody and immunohistochemical detection.** A custom anti-NHX-2 antibody was raised in rabbits against the peptide CNDGFENDGYEDES and was affinity purified (Invitrogen, Carlsbad, CA). Whole worm fixation was performed using a standard peroxide tube protocol. Antibody dilutions in standard detection buffer (PBS-Tween 20) were as follows: 1:250 rabbit anti-NHX-2 and 1:1,000 goat anti-rabbit Alexa555 (Molecular Probes/Invitrogen). For V5 epitope detection, a mouse anti-V5 antibody (Invitrogen) was used at 1:2,000 with secondary detection using a goat anti-mouse Alexa555 as above. Worms were mounted on cover slips in Fluoromount G (Southern Biotech), sealed, and imaged by fluorescence microscopy.

Alternatively, RT311 (GFP::RAB-11) worms were treated with *pbo-1* RNAi for two generations; 10–15 adult hermaphrodites were put in 5 μl M9 solution on poly-L-lysine-coated slides. The intestines of adult hermaphrodites were gently exposed by using a 26-gauge syringe needle to pierce the cuticle, allowing the gonads and intestines to extrude from the animals. Worms were fixed by 2% formaldehyde with 50% methanol in PBS and incubated at room temperature for 30 min in a humidified chamber. After fixation and subsequent washing with PBS containing 0.1% BSA with 0.5% Triton X-100, worms were incubated with mouse anti-GFP (monoclonal antibody; Clontech) and rabbit anti-NHX-2 antibodies for 2 h at room temperature in a humidified chamber, washed again, and then incubated with secondary goat anti-mouse or goat anti-rabbit Alexa antibodies for 30 min at room temperature. Antibody dilutions were 1:250 for NHX-2, 1:1,000 for GFP, and 1:1,000 for goat anti-rabbit Alexa555 and goat anti-mouse Alexa488. The final specimens were mounted on cover slips for imaging in Fluoromount G (Southern Biotech).

## RESULTS

**Both basolateral and apical NHE require PBO-1 for membrane targeting or stability.** The *C. elegans* CHP family member *pbo-1* has been shown to regulate intestinal NHE activity (51), and mutation of the PBO-1-binding domain in the basolateral NHE NHX-7 suppresses its ability to function (3). To examine the underlying mechanism, an NHX-7::mCherry-tagged fusion protein was expressed via the native *nhx-7* promoter in transgenic worms, and its distribution was assessed by confocal microscopy. To avoid overexpression artifacts, qRT-PCR was used to identify transgenic lines that expressed the transcript coding for the recombinant protein at close to endogenous levels (data not shown). In a wild-type genetic background, the fusion protein colocalized with a fluorescent extracellular (EC) pH sensor fused to the aquaporin 5 basolateral targeting motif (3) (Fig. 1, A and B). However, in a *pbo-1(tm3716)* loss-of-function background, which is both smaller and has a morphologically distinct intestine, the NHX-7::mCherry fusion protein instead accumulated inside of the intestinal cells (Fig. 1D), even though the EC sensor was targeted to the basolateral membrane correctly (Fig. 1E). NHX-7::mCherry mistargeting was also observed in specimens subjected to *pbo-1* RNAi (Fig. 1, F and G) and in a second less-affected *pbo-1* mutant, the *sa7* allele, which contains a substitution of E135K that reverses the charge of a highly conserved residue in the third EF hand (Fig. 3D). qRT-PCR

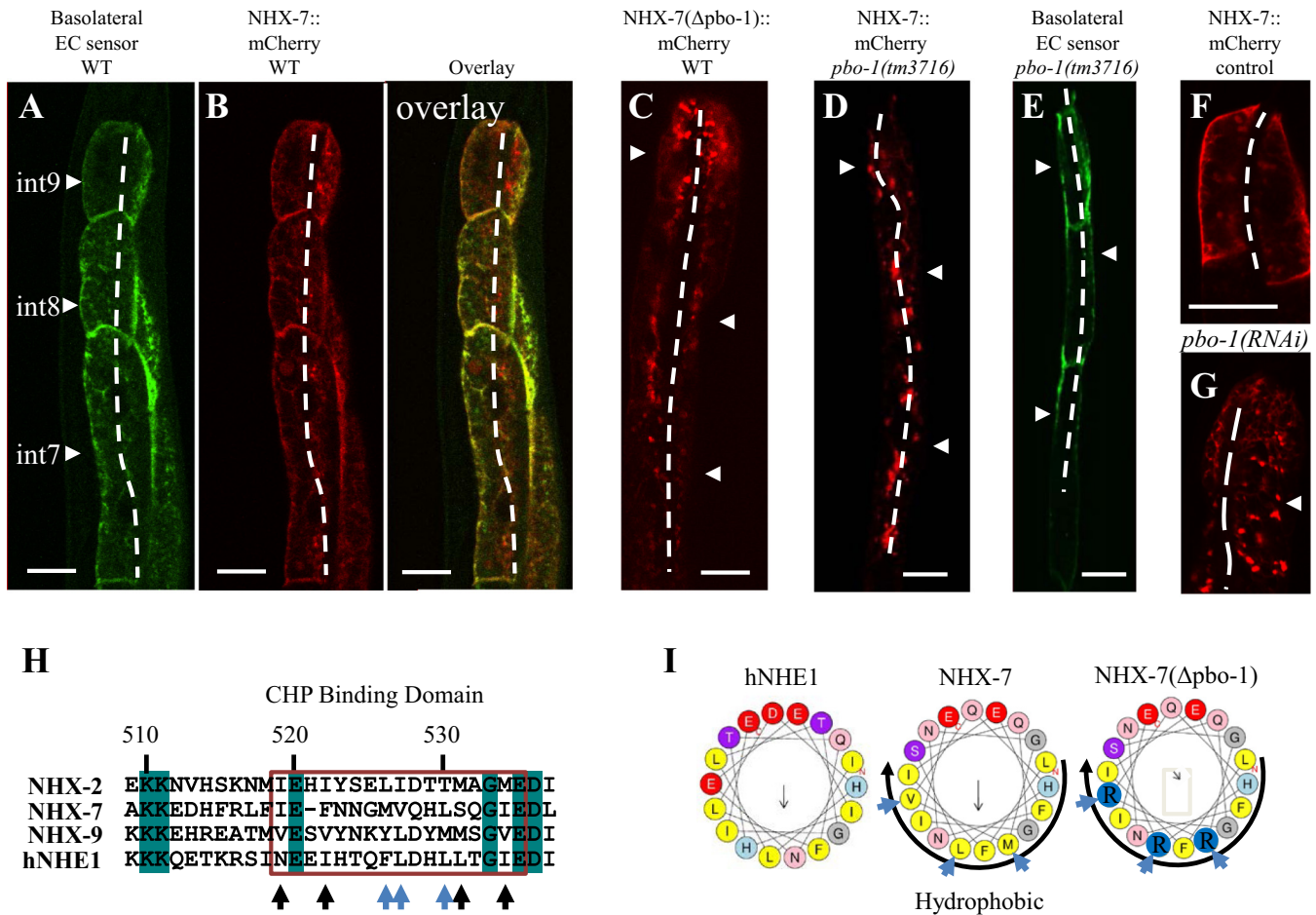


Fig. 1. PBO-1 promotes plasma membrane localization of the Na<sup>+</sup>/H<sup>+</sup> exchanger (NHE) NHX-7 in live worms. The expression of a recombinant, low-copy NHX-7::mCherry fusion protein was assessed by confocal microscopy in live immobilized transgenic animals. White arrowheads denote the basolateral membrane of posterior intestinal cells int7, -8, and -9 where NHX-7 is expressed, and dotted lines approximate the intestinal lumen. *A* and *B*: an extracellular (EC) pH sensor marks the basolateral membrane (*A*) where wild-type NHX-7::mCherry clearly resides (*B*). *C*: mutation of the PBO-1-binding domain in NHX-7(Δpbo-1) results in redistribution of the exchanger from the basolateral membrane to intracellular organelles and/or aggregates. *D*: wild-type NHX-7 displays a similar distribution in a *pbo-1(tm3716)* mutant background as NHX-7(Δpbo-1) does in a wild-type genetic background. *E*: plasma membrane targeting of the recombinant EC pH sensor is unaffected by the loss of *pbo-1*. *F* and *G*: wild-type NHX-7::mCherry distribution is altered (*F*) following RNA interference (RNAi)-mediated knockdown of *pbo-1* (*G*). The images in *A* and *B* are from the same worm, imaged in the green and red spectrum, with the overlay shown as indicated. All other images are individual worms. Please note that the acquisition parameters were identical for *B*, *C*, *D*, *F*, and *G* and that the *pbo-1(tm3716)* mutants are quite small and sickly. Scale bars are 20 μM. *H*: protein sequence alignment of worm NHX proteins with the rat NHE1 amino acids 509–537. The calcineurin B homologous proteins (CHP)-binding region is bound by a red box. Blue shading indicates sequence identity. Arrows denote key residues positioned on the hydrophobic face in the mammalian exchanger, several of which have been colored blue to indicate specific amino acids that were mutated to disrupt PBO-1 binding. These mutations were based upon the approach used to disrupt CHP1 binding to mammalian NHE1, -2, and -3 by Pang et al. (43). *I*: HeliQuest was used to generate alpha helical wheel projections from the sequence alignment shown in the boxed region in the alignment. The internal arrow indicates the hydrophobic moment, and its size corresponds to its overall hydrophobicity. The hydrophobic face of the predicted amphipathic alpha helix in NHX-7 is represented by a curved black arrow, and the amino acids that were mutated are indicated by blue arrows, as in *H*.

confirmed >90% reduction in *pbo-1* transcript levels following RNAi (data not shown). Finally, both the *pbo-1* RNAi worms and the *pbo-1(sa7)* mutants were slightly healthier than *pbo-1(tm3716)* mutant worms, consistent with the effect of knockdown or a hypomorphic allele, respectively, vs. a complete loss-of-function in the *tm3716* mutant.

Mammalian CHP1 belongs to a multifunctional protein family (18) that has been suggested to contribute to protein trafficking (6, 8). Hence, it is possible that the NHX-7-targeting phenotype could arise indirectly. To circumvent this, we mutated three residues in a region of the *nhx-7* coding sequence as shown in Fig. 1*H* (M541R/V542R/L545R) that disrupts an amphipathic alpha helix that is structurally important for the interaction between NHE/CHP (Fig. 1*I*). Although we did not

verify biochemically that the interaction with PBO1 was disrupted in the mutant, the same mutations in mammalian NHE1, NHE2, and NHE3 have been shown to suppress binding to CHP1 (43).

Like wild-type NHX-7 in a *pbo-1(tm3716)* genetic background, the mutated NHX-7(Δpbo-1)::mCherry fusion protein accumulated in the cytoplasm, even in a wild-type genetic background (Fig. 1*C*), and our previous work showed that this mutant was unable to complement the *pbo* defect in an *nhx-7(ok583)* loss-of-function mutant (3). Unlike the *pbo-1* mutant, however, these worms were otherwise healthy. Together, these results suggest that PBO-1 contributes to NHX-7 membrane targeting or retention, that binding of PBO-1 to NHX-7 is important for this function, and that the adverse phenotypes

displayed by the *pbo-1(tm3716)* mutant arise independent of NHX-7. In addition, we found that a V5-PBO-1 transgenic protein, which rescues the *pbo* mutant phenotype (data not shown), is mainly cytoplasmic but is not distributed diffusely through the cell (Fig. 3E). Instead, the punctate distribution appears consistent with it being associated with intracellular organelles. As a caveat, this distribution may reflect overexpression, but at face value provides some support for PBO-1 being important for trafficking.

NHX-2 is an apical NHE that contributes to the worm's viability through its physiological coupling to nutrient transporters (39, 40). NHX-2 also contains a predicted binding site for PBO-1 (Fig. 1H). The starvation phenotype of *pbo-1* mutants and the physiological impact of *pbo-1* loss on proton flux across the apical membrane (51) support a role for PBO-1 in regulating NHX-2 activity.

Unfortunately, transgenic lines expressing fluorescent NHX-2 fusion proteins were not sufficiently bright for our purposes. Hence, we developed a custom anti-NHX-2 antibody and applied the affinity-purified antibody to samples fixed for immunohistochemistry. The antibody bound robustly to a target in the apical membrane of the intestine in wild-type worms (Fig. 2A) but not in worms treated with *nhx-2* RNAi (Fig. 2A, inset). As predicted, the *pbo-1(tm3716)* mutant accumulated

NHX-2 in the cytoplasm rather than at the membrane (Fig. 2C), although its distribution was markedly different from the NHX-7 (Fig. 1, C and D). Moreover, RNAi of *pbo-1* resulted in a similar staining pattern (data not shown). However, when the antibody was applied to samples of *pbo-1(sa7)* mutants, NHX-2 labeling persisted at the apical membrane, resembling its wild-type distribution (Fig. 2B). This suggested that the physical presence of the mutant PBO-1(sa7) protein is sufficient for membrane stabilization of the NHE, even if it does not appear to support robust NHX-2 activity (51). However, given the resolution of the technique, it is also possible that NHX-2 is subapical in the *sa7* mutant. Finally, not all intestinal NHE proteins require PBO-1 for targeting, since an NHX-4::mCherry fusion was found to be distributed normally to the basolateral membrane following *pbo-1* (RNAi) (Fig. 2, E and F), and not all apical transporters are affected either, since the apical V-ATPase subunit VHA-6 (2) was also correctly targeted following either *pbo-1* (RNAi) or in a *pbo-1(sa7)* mutant (Fig. 2D). The NHX-4::mCherry transgene was normally distributed in the *pbo-1(sa7)* mutant as well (data not shown).

*PBO-1 targeting of intestinal NHEs.* *C. elegans* has been used extensively as a genetic model to study intracellular trafficking, and there are a variety of strains expressing fluorescent transgenic fusions that label individual organelles (12,

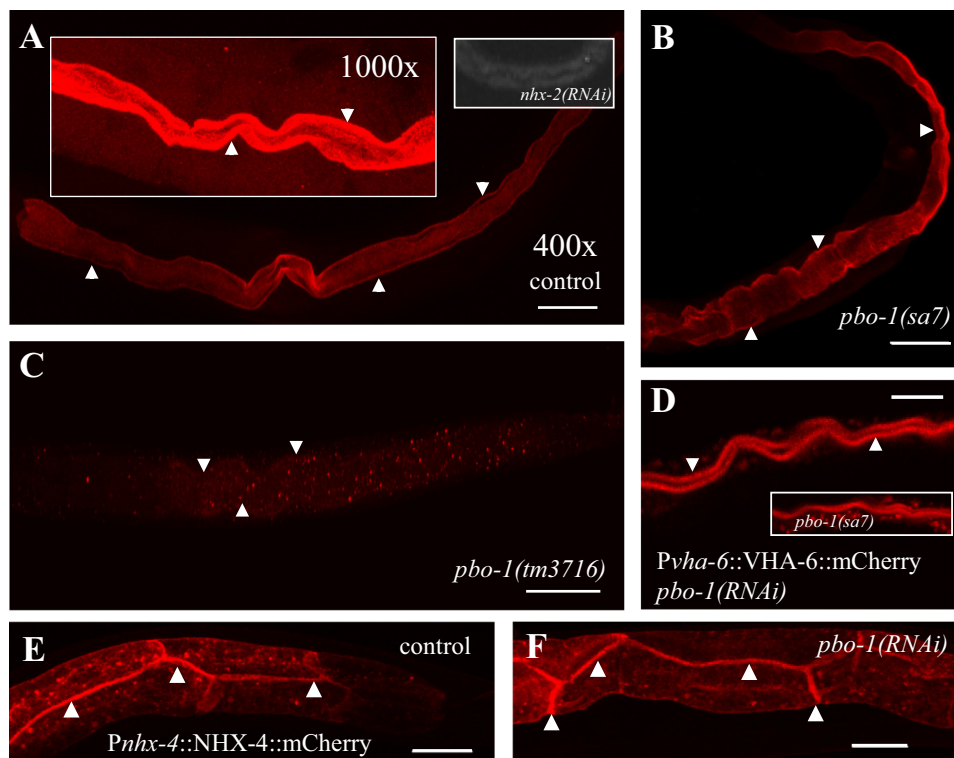


Fig. 2. PBO-1 regulates NHX-2 function and retention at the apical membrane through separable mechanisms. Endogenous NHX-2 was detected with a custom-generated antibody raised against the sequence NH3-CNDGFENDGYESDES-COOH in the extreme COOH-terminus of NHX-2 protein. Antibody target recognition was visualized with an Alexa 555-conjugated secondary antibody via fluorescent micrography. White arrowheads indicate the intestinal apical membrane. A: control worms, at  $\times 400$  and  $\times 1,000$  magnification, as well as negative control *nhx-2*(RNAi) worms, shown in the inset on right. The exposure time was increased 10-fold for the *nhx-2*(RNAi) worms so as not to present a blank picture; the resulting signal was limited to autofluorescence, and the lumen/apical membrane is clearly not detected. B and C: *pbo-1(sa7)* missense mutant worms (B) and *pbo-1(tm3716)* null worms (C). D: confocal fluorescent micrograph of transgenic *Pvha-6::VHA-6::mCherry* protein expression in a live anesthetized *pbo-1*(RNAi) worm. Inset shows *Pvha-6::VHA-6::mCherry* in the *pbo-1(sa7)* mutant background. E and F: confocal fluorescent micrographs of transgenic *Pnhx-4::NHX-4::mCherry* protein expression in live anesthetized control and *pbo-1*(RNAi) worms, as labeled. White arrowheads denote labeling of the intestinal basolateral and lateral membranes, with the cell junctions being most readily visible. The scale bars are as follows: 5  $\mu$ M (A–C), 20  $\mu$ M (D), and 20  $\mu$ M (E and F). The inset in A was acquired using a higher-magnification objective, as shown.

47). To determine where NHX-7 was targeted in the absence of PBO-1 binding, these marker alleles were crossed into strains expressing mutant NHX-7, and their relative distribution was assessed via confocal microscopy. The NHX-7( $\Delta$ pbo-1)::mCherry fusion protein colocalized with GFP::RAB-7 in the intestine, which was used to mark late endosomes and lysosomes (11, 34, 50) (Fig. 3, A and B), but not with AMAN-2-, RAB-5-, or RAB-10-positive vesicles, which represented endoplasmic reticulum/Golgi, early endosomes, or basolateral recycling endosomes, respectively (data not shown). The reciprocal finding that the wild-type NHX-7::mCherry fusion protein also colocalized with RAB-7::GFP vesicles in a *pbo-1(lf)* genetic background (Fig. 3D) confirmed that PBO-1 binding prevents default targeting of NHX-7 to late endosome/lysosomes and suggests that the lysosomal localization is not merely a secondary result of protein misfolding.

Characteristic blue intestinal autofluorescence normally found in terminal lysosomes (or “gut granules”) (14) is comprised of anthranilic acid glucosyl esters and localized with some but not all of the labeled vesicles (Fig. 3C). This suggests that NHX-7::mCherry may be present in an overlapping subset of RAB-7(+)/anthranilic acid(+) vesicles. The appearance of both the wild-type NHX-7::mCherry and NHX-7( $\Delta$ pbo-1)::mCherry fusion protein inside the vesicle lumen (Fig. 3, B and D) suggested that the COOH-terminal mCherry tag may have been cleaved from NHX-7, which would be expected to reside in the membrane.

In the case of NHX-2, we speculated based upon the juxtaluminous distribution observed in the *pbo-1(tm3716)* mutant and the fact that regulation of apical NHEs such as NHE3 in mammals often occurs through membrane insertion and retrieval from recycling endosomes (52) that the NHX-2<sup>+</sup> labeling observed in the *pbo(-)* strains represented apical recycling

endosomes. In worms, these organelles can be defined by RAB-11::GFP labeling. Our initial observations with live transgenic worms expressing this marker indicated that the apical recycling endosomes were slightly disorganized in live animals treated with *pbo-1* RNAi (Fig. 4, B and C). This is consistent with an established role of the mammalian CHP1 being a calcium-dependent signal protein mediating organelle assembly with the microtubule to affect protein trafficking (5, 8).

Unfortunately, the standard immunohistochemistry fixation protocol used in Fig. 2 to disrupt the worm’s cuticle suppressed both GFP fluorescence and detection by commercial anti-GFP antibodies (data not shown). Hence, to test whether NHX-2 colocalized with the apical recycling endosomes as predicted, a physical exposure of the intestine was accomplished by gently slicing open the worm’s cuticle. This caused part of the intestine to extrude from the body cavity, as shown in Fig. 4D. A brief fixation period was followed by antigen detection using anti-GFP and anti-NHX-2 antibodies. This method resulted in robust detection of both epitopes, with a tissue morphology that was more akin to live worms than to fixed worms and better labeling of intracellular NHX-2 itself.

Counter to our prediction, in *pbo-1(RNAi)* worms only rarely did the NHX-2<sup>+</sup> organelles (Fig. 4, E and H) colocalize with the GFP<sup>+</sup> apical recycling endosomes (Fig. 4, F and I). In confocal projections of luminal cross sections (Fig. 4, E–G) or in more peripheral cytoplasmic areas of the intestine (Fig. 4, H–J), there were occasional areas of overlap between the two labels (Fig. 4, G and J), but it seems clear that the vast majority of labeled puncta are mutually exclusive. At present, the identity of the NHX-2<sup>+</sup> structures is unknown.

*C. elegans* code for two paralogs of *pbo-1*. Using BLAST to search the *C. elegans* genome, two predicted protein coding

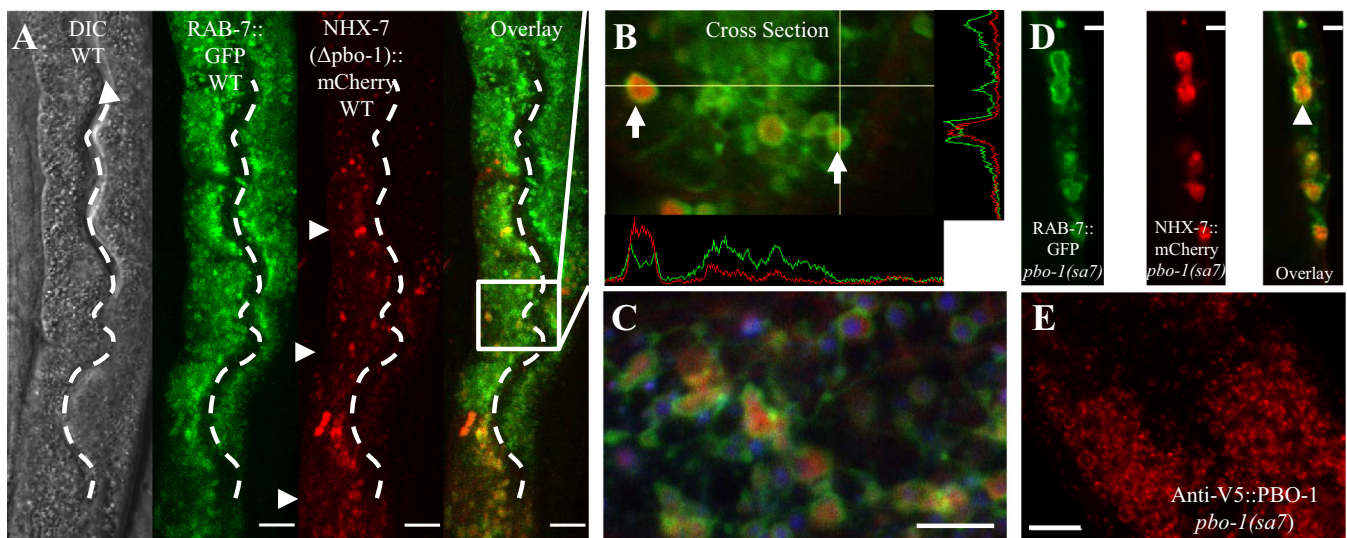
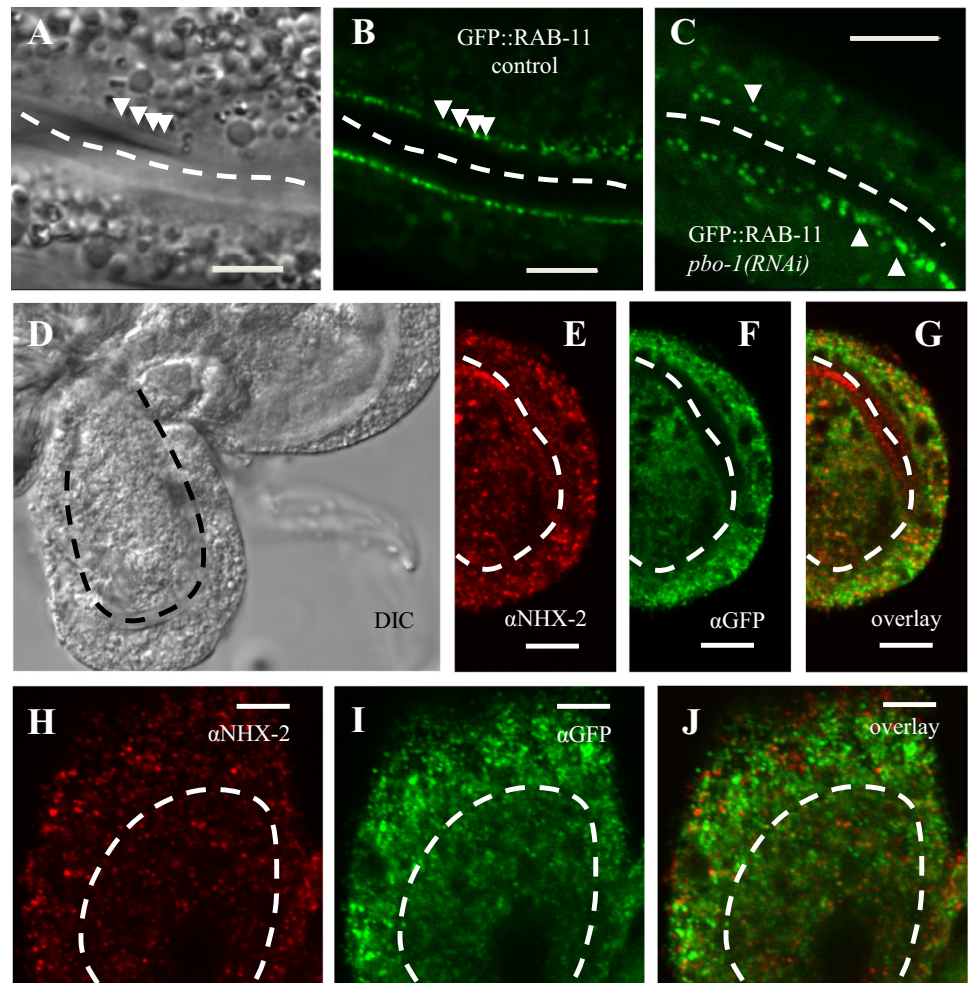


Fig. 3. Loss of PBO-1 binding causes NHX-7 to accumulate in late endosomes/lysosomes. Confocal micrographs of fluorescent protein expression. A: NHX-7( $\Delta$ pbo-1)::mCherry expression in a strain in which intestinal late endosome/lysosomes are labeled with green fluorescent protein (GFP) via an integrated translational fusion to RAB-7 protein. The arrow in the differential interference contrast (DIC) image orients the worm and is pointing toward the head. The white arrowheads in the NHX-7( $\Delta$ pbo-1)::mCherry image denote the basolateral membrane of int7, -8, and -9. B: a cross section magnified from the overlap as shown confirms mCherry protein in GFP-positive vesicles, quantified by horizontal and vertical histograms. The white arrowheads indicate vesicles of interest through which the histograms were obtained, as shown. C: NHX-7( $\Delta$ pbo-1)::mCherry(+), RAB-7(+) vesicles coincide with anthranilic acid glucosyl ester(+) gut granules, or terminal lysosomes. D: wild-type NHX-7 fusion protein expressed in the *pbo-1(sa7)* background colabels RAB-7::GFP(+) late endosome/lysosomes. Scale bars are 10  $\mu$ M. E: confocal micrographs of V5::PBO-1 expression detected with an anti-V5 antibody and visualized with an Alexa 555-conjugated secondary. Scale bar is 5  $\mu$ M.

Fig. 4. PBO-1 protein stabilizes NHX-2 at the apical membrane. DIC (A) and fluorescent confocal micrograph (B) of recycling endosomes labeled via a GFP::RAB-11 fusion in control RT311 and in *pbo-1(RNAi)* RT311 worms (C). The worms were imaged live under anesthetic restraint. White arrowheads are adjacent to the lumen and highlight GFP::RAB-11-positive apical recycling endosomes. D: DIC image of the intestinal preparation used for immunolabeling, with part of the intestine extruding as a loop after gently slicing the worm's cuticle. E–J: fluorescent detection of endogenous NHX-2 protein and a transgenic GFP::RAB-11 marker of apical recycling endosomes in fixed *pbo-1(RNAi)* worms, using anti-NHX-2 and anti-GFP antibodies as labeled. The lumen is denoted by a dotted white line. Scale bars are 5  $\mu$ M.



regions were identified with significant homology to PBO-1. These proteins also shared homology with the three mammalian CHP family members, and like those proteins exhibited some hallmark motifs conserved in key regions such as Ca<sup>2+</sup>-binding EF hands, NH<sub>2</sub>-terminal myristoylation motifs, and predicted nuclear export signals (Fig. 5). Based upon the likelihood of their interaction with other NHEs in worms, we examined their expression patterns for overlap with the nine worm NHEs (40).

The first of these was encoded by ZK856.8, heretofore known as calcineurin-like EF-hand protein family member *chpf-1*. Its genomic coding region is the last in an operon consisting of six genes, which also codes for a zinc finger protein, a transcription factor, an RNA pol III subunit, and two other uncharacterized gene products (Fig. 6A). Approximately 17% of the genes in *C. elegans* are contained in operons (1). Trans-splicing of one of two short leader RNAs, SL1 or SL2, occurs at the 5'-ends of pre-mRNAs of many *C. elegans* genes, with SL2 leaders characteristic of mRNAs expressed from operons. In the case of *chpf-1*, both SL1 and SL2 leaders were identified on the mature mRNA. This suggested that *chpf-1* expression can be driven by both the operon promoter and the intercistronic region just upstream of its coding sequence. Interrogating the individual expression patterns of each of these promoter regions suggested a mutually exclusive distri-

bution, with the operon promoter widely expressed in hermaphrodites, particularly in muscle cells (Fig. 6B), and the small intercistronic promoter expressed solely in males in unidentified cells (Fig. 6C). These results should be interpreted with the caveat that transgenic expression patterns do not necessarily reflect the endogenous distribution of native genes and contain neither the genomic coding sequence nor 3'-untranslated region. However, the widespread expression of *chpf-1* from the operon promoter is consistent with a housekeeping role.

The second gene was coded for by F59D6.7 and named *chpf-2*. It is expressed from a single promoter (Fig. 6D) expressed solely in the excretory cell of hermaphrodites (Fig. 6E). This long, H-shaped cell extends canal-like processes along the basolateral surface of the hypodermis and contributes to systemic osmoregulation and waste removal. In males, the *chpf-2* promoter also drove expression in the ray support cells (Fig. 6F). These cells arise postembryonically during morphogenesis of the male tail, which in worms is a sensory organ involved in mating behaviors. Interestingly, NHX-9 is also expressed specifically in the excretory cell (40). Hence, we tested the hypothesis that *chpf-2* regulation of *nhx-9* contributes to excretory cell function.

*Loss of chpf-2 impacts excretory cell function.* The excretory system in worms works much like the mammalian renal system

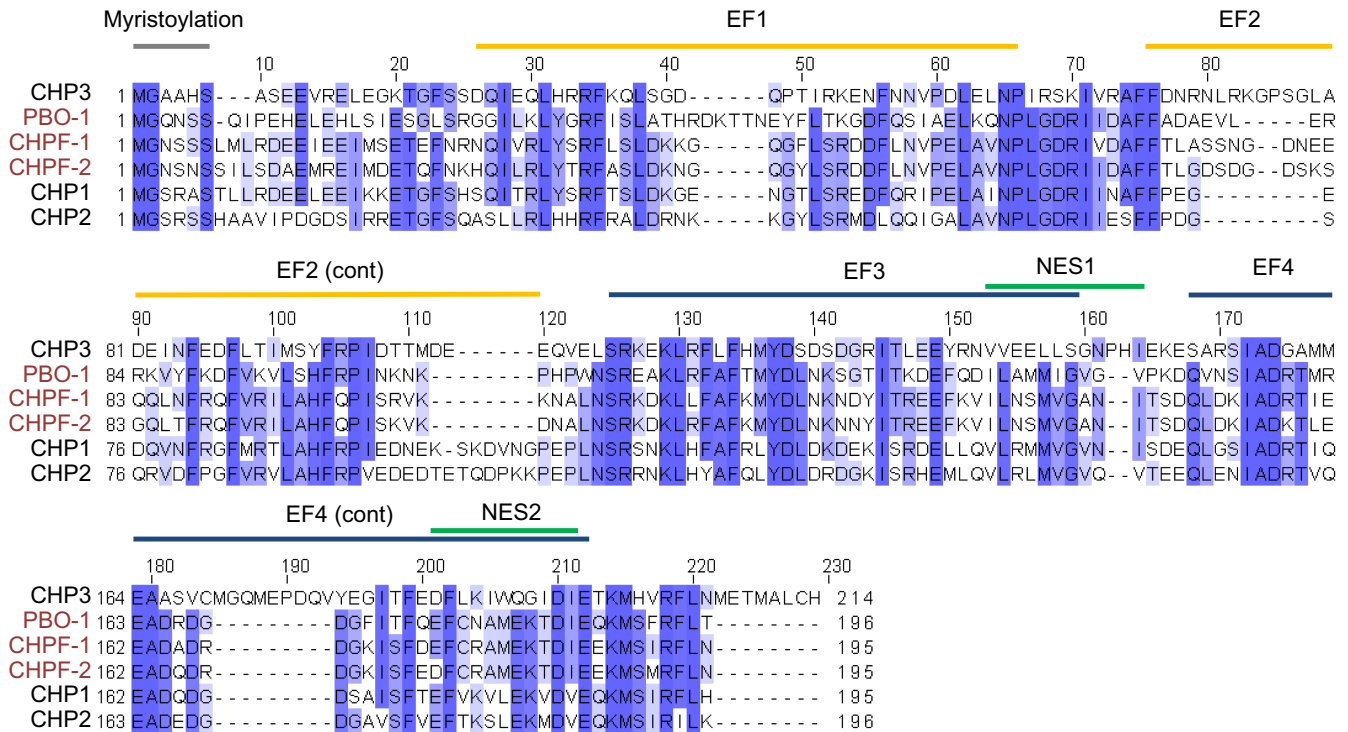


Fig. 5. Sequence alignment of *Caenorhabditis elegans* and human CHP family proteins. Analysis was performed using ClustalW 2 and formatted using Jalview. Shading indicates sequence identity from low (light blue) to high (dark blue). Structural domains are labeled accordingly, based on mammalian studies, and designated by colored lines. Worm protein names are in red. EF, EF-hand helix-loop-helix; NES, nuclear export signal.

in osmoregulation and waste removal. When worms are moved to high-salt plates, hypertonic shrinkage occurs but is readily compensated for by the accumulation of organic osmolytes through defined molecular signaling pathways (13, 25). Subsequently, moving the high-salt adapted worms to low-salt plates induces hypotonic stress which requires excretory cell function to mediate systemic regulatory volume decreases, and laser ablation of the excretory cell results in fluid retention and death (41).

To test the role of *chpf-2* in excretory cell function, we obtained a mutation in *chpf-2* that had been generated by the *C. elegans* Gene Knockout Consortium. The *chpf-2(ok2941)* allele has a 600-nucleotide deletion that removes more than one-half of the coding sequence (Fig. 6D) and likely results in a complete loss-of-function. Because the deletion boundaries are contained within the genomic coding sequence, it is unlikely to impact surrounding genes. Our results demonstrate that the *ok2941* mutant exhibited ~20% reduced survival compared with control worms after recovery from high-salt exposure, suggesting a deficiency in excretory cell function (Fig. 7A). There was no deficit noted upon the initial transfer to high salt (data not shown), suggesting that this was not a general defect in osmotic adaptation. Moreover, the general morphology of the excretory cell, as judged by wCherry labeling, appeared to be normal in the *ok2941* genetic background (Fig. 7B).

The NHE family member *nhx-9* is expressed strongly in the excretory cell (40), and the NHX-9 protein contains a CHP family binding motif (Fig. 1H) that is predicted to form an amphipathic alpha helix (data not shown). If NHX-9 were to interact with CHPF-2 in a mechanistically similar way as PBO-1 does with the intestinal NHEs, it would be reasonable

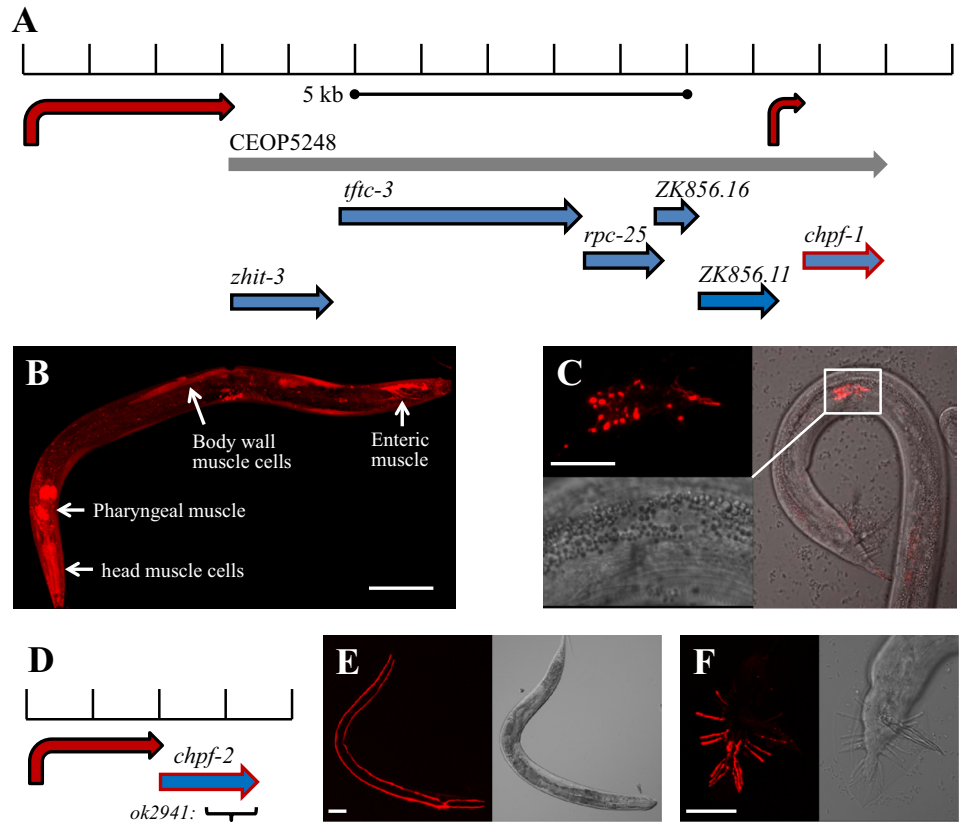
to predict that NHX-9 would be mislocalized in the *ok2941* mutant.

This prediction was tested by examining the distribution of an NHX-9::GFP translational fusion protein in the excretory cell of wild-type and *ok2941* mutants (Fig. 8C). While it is not currently known whether NHX-9 normally localizes to the apical or basolateral cell surface, it was immediately obvious that there were not gross differences in the distribution of NHX-9 protein in these genetic backgrounds. However, over-expression of NHX-9::GFP from the transgenic array could occlude normal regulatory mechanisms. Moreover, the excretory cell is polarized around a central lumen where the canals are quite small, and it is possible that subtle differences such as movement in apical recycling endosomes from the apical membrane would be undetected. More informative, however, was the finding that *nhx-9(ok847)* deletion mutants exhibited normal responses to hypotonic challenge (Fig. 7A). Hence, it is not likely that any suspected redistribution of NHX-9 protein in the CHP family *ok2941* mutant would result in measureable consequences, regardless. We conclude that the *ok2941* mutant likely exerts its effect through another NHE or a separate mechanism entirely.

DISCUSSION

CHP family proteins vary in their structural elements and expression profiles, but are similar in that they all have been shown to bind to and regulate NHEs. However, the mechanism through which these proteins exert their effect has been obscured by conflicting results. It has been suggested that CHP protein binding is necessary for NHE ion transport, biosyn-

Fig. 6. Calcineurin-like EF-hand protein family member (*chpf-1* and *chpf-2* expression profile. **A**: schematic of the genomic region containing the *chpf-1* gene (blue arrow outlined in red). *Chpf-1* is the last gene in the operon CEOP5248 (gray arrow). The other genes in the operon are depicted as blue arrows. The promoter regions used to drive wCherry expression in **B** and **C** are depicted by solid red arrows. **B** and **C**: fluorescent micrographs of transgenic worms expressing wCherry from either the upstream operon promoter, which is widely expressed throughout the body of hermaphrodites (**B**), or the small intergenic promoter, which is only expressed in males (**C**), in unidentified cells. Scale bars are 50 μM. **D**: schematic of the *chpf-2* gene, whose promoter and genomic coding sequences are depicted as described in **A**. The limits of the *chpf-2(ok2941)* deletion are denoted by a black brace. **E** and **F**: fluorescent and DIC images of transgenic worms expressing *chpf-2* promoter::wCherry fusions. The hermaphrodite in **E** exhibits excretory cell-specific expression, which is a large H-shaped cell with canals that extend on either side of the body. The male in **F** exhibits specific expression in cells of the male ray, which is involved in mating behavior. Scale bars are 50 and 10 μM, respectively.



thetic maturation, trafficking to the membrane, or membrane stability, and that these are influenced by CHPs independently, in aggregate, or not at all (for review, see Ref. 18). A recent consensus seems to be that individual functions may be cell type specific as well as specific for the individual CHP and NHE paralogs in question.

Worms have a similar genomic complexity in the NHE and CHP gene families, with nine and three paralogs each, respectively. Here, we took advantage of the genetic reagents, the limited repertoire of tissues, and stereotypical behaviors in worms to decipher how CHP function in one tissue can influence multiple NHEs. Previous work has

shown that the *C. elegans* CHP family protein PBO-1 is expressed in the intestine and contributes to intestinal NHE activities (3, 51). Our results suggest surprising differences in how each of these NHEs reacted to the loss of PBO-1. In the case of NHX-7, of the three approaches taken (deleting the *pbo-1* gene, mutating a single residue in the *pbo-1* coding region, or removing the PBO-1-binding site in NHX-7 itself) all resulted in a similar outcome: NHX-7 was targeted to late endosomes/lysosomes. Hence, a physical association between NHX-7 and PBO-1 as well as functional PBO-1 calcium-binding activity are both required for proper targeting.

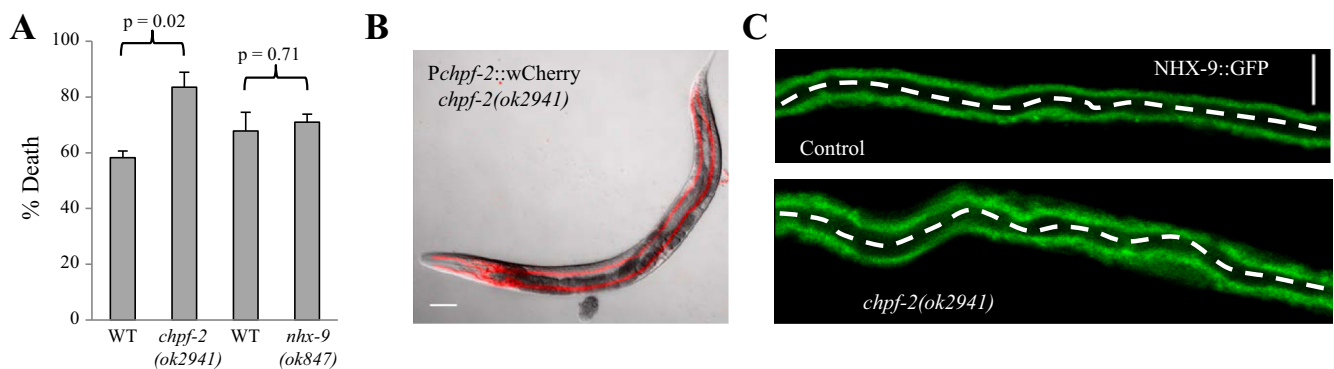


Fig. 7. *Chpf-2* impacts excretory cell function. **A**: worms were allowed to acclimate to hyperosmotic conditions for 24 h before moving them back to normosmotic media. Survival was assayed following 12 h of recovery. Values are averages of 3 paired trials with a minimum of 25 worms/trial. Significance was determined using a two-sample *t*-test. **B**: wCherry labeling of the H-shaped excretory cell in *chpf-2(ok2941)* mutants indicates normal gross morphology. Scale bar is 50 μM. **C**: NHX-9::GFP expression in the excretory cell of wild-type worms (*top*) or *chpf-2(ok2941)* mutant animals (*bottom*). The excretory cell lumen is denoted by a white dotted line. The scale bar, which is oriented vertically, is 5 μM.

In contrast, the distribution of NHX-2 differed dramatically in the two genetic *pbo-1* mutant backgrounds. In the deletion mutant, NHX-2 was mistargeted and accumulated in the cell (Fig. 4). However, in the missense mutant, NHX-2 was found at the plasma membrane. These differences suggested that physical binding of PBO-1 to NHX-2 suffices for membrane stability. We have previously shown that *sa7* is a strong loss-of-function allele and phenocopies *nhx-2(lf)* (51). Thus, PBO-1 calcium binding is likely necessary for robust NHE activity, if not for membrane stability. We note that mammalian NHE3 regulation by CHP1 has been proposed to increase NHE3 constitutive transport function, protein abundance, and regulation by calcium (16, 17, 19), but that the precise mechanisms underlying this regulation are complicated and may reflect interactions with adaptor proteins or specific settings. NHX-2 contains several motifs predicted to interact with adaptor proteins, which serve to direct trafficking within the endosomal and secretory pathways, one of which falls in the middle of the PBO-1-binding domain. It is possible that this motif is masked in the presence of PBO-1. Alternatively, perhaps a regulatory motif is unmasked by PBO-1 calcium binding. Within this context, it is intriguing to speculate that NHX-2's trafficking might be coupled to calcium signaling, given that intestinal calcium oscillations occur frequently with an ~50-s period (15). It is also possible that other interactions, such as with ERM proteins as has been shown to be important for NHE3 signaling (16), may contribute to this process, and new evidence is emerging that CHP1 can regulate the exchanger set point for pH<sub>i</sub> (7).

In addition to PBO-1 in the intestine, we have also reported the presence of two additional CHP isoforms, *chpf-1* and *chpf-2*. Based simply upon sequence homology and protein motif analysis, we were unable to predict which worm paralog is orthologous to a particular mammalian CHP family protein. It is interesting to note, however, that the expression of both PBO-1, the first characterized worm CHP family member (51), and *chpf-2* is quite restricted compared with *chpf-1*. This is also true for the limited tissue expression profile of mammalian CHP2 and CHP3 compared with CHP1 (18).

Our results demonstrating that *chpf-2(lf)* mutants were not as effective at surviving hypotonic exposure suggested a problem with water balance and a defect in excretory cell function (Fig. 7). However, a strain lacking expression of the excretory cell-specific NHX-9 responded to hypotonic exposure normally, suggesting that NHX-9 is an unlikely candidate to contribute to the *chpf-2(lf)* mutant phenotype. It is possible that CHPF-2, like CHP1 in mammals, may participate more generally in organelle trafficking and that the mutant phenotype arises from this aspect of its function. Alternatively, there may be another NHE whose loss causes an excretory cell defect.

In conclusion, previous studies have suggested that CHP's regulation of NHEs is mechanistically complex, and the results presented here suggest a similar complexity is conserved in a simple genetic model organism. The availability of genetic resources, including viable loss-of-function mutants, should help to unravel this complexity.

#### ACKNOWLEDGMENTS

Several strains were provided by the *C. elegans* Gene Knockout Consortium, the Japanese National Bioresource Project, and the *C. elegans* Genetics

Center, which is funded by NIH Office of Research Infrastructure Programs (P40 OD010440). We thank Teresa Sherman, whose help has been invaluable over the years, Jamie Wagner, who began the *pbo-1* project at Oberlin College as an undergraduate student, and Dr. Barth Grant for discussions and guidance.

#### GRANTS

This work was supported in part by National Science Foundation Grants IOS 0919848 and IOS 1352836 to K. Nehrke and IOS 0842830 to M. A. Peters.

#### DISCLOSURES

No conflicts of interest, financial or otherwise, are declared by the authors.

#### AUTHOR CONTRIBUTIONS

Author contributions: E.A., M.A.P., and K.N. conception and design of research; E.A., Q.W., R.L.W., and M.A. performed experiments; E.A., Q.W., R.L.W., M.A., and K.N. analyzed data; E.A., Q.W., R.L.W., M.A., and K.N. interpreted results of experiments; E.A. and K.N. prepared figures; E.A., Q.W., M.A.P., and K.N. drafted manuscript; E.A., Q.W., R.L.W., M.A., M.A.P., and K.N. approved final version of manuscript; Q.W., M.A.P., and K.N. edited and revised manuscript.

#### REFERENCES

- Allen MA, Hillier LW, Waterston RH, Blumenthal T. A global analysis of *C. elegans* trans-splicing. *Genome Res* 21: 255–264, 2011.
- Allman E, Johnson D, Nehrke K. Loss of the apical V-ATPase  $\alpha$ -subunit VHA-6 prevents acidification of the intestinal lumen during a rhythmic behavior in *C. elegans*. *Am J Physiol Cell Physiol* 297: C1071–C1081, 2009.
- Allman E, Waters K, Ackroyd S, Nehrke K. Analysis of Ca<sup>2+</sup> signaling motifs that regulate proton signaling through the Na<sup>+</sup>/H<sup>+</sup> exchanger NHX-7 during a rhythmic behavior in *Caenorhabditis elegans*. *J Biol Chem* 288: 5886–5895, 2013.
- Ammar YB, Takeda S, Hisamitsu T, Mori H, Wakabayashi S. Crystal structure of CHP2 complexed with NHE1-cytosolic region and an implication for pH regulation. *EMBO J* 25: 2315–2325, 2006.
- Andrade J, Pearce ST, Zhao H, Barroso M. Interactions among p22, glyceraldehyde-3-phosphate dehydrogenase and microtubules. *Biochem J* 384: 327–336, 2004.
- Andrade J, Zhao H, Titus B, Timm Pearce S, Barroso M. The EF-hand Ca<sup>2+</sup>-binding protein p22 plays a role in microtubule and endoplasmic reticulum organization and dynamics with distinct Ca<sup>2+</sup>-binding requirements. *Mol Biol Cell* 15: 481–496, 2004.
- Babich V, Vadnagara K, Di Sole F. The biophysical and molecular basis of intracellular pH sensing by Na<sup>+</sup>/H<sup>+</sup> exchanger-3. *FASEB J* 27: 4646–4658, 2013.
- Barroso MR, Bernd KK, DeWitt ND, Chang A, Mills K, Sztul ES. A novel Ca<sup>2+</sup>-binding protein, p22, is required for constitutive membrane traffic. *J Biol Chem* 271: 10183–10187, 1996.
- Beg AA, Ernststrom GG, Nix P, Davis MW, Jorgensen EM. Protons act as a transmitter for muscle contraction in *C. elegans*. *Cell* 132: 149–160, 2008.
- Brenner S. The genetics of *Caenorhabditis elegans*. *Genetics* 77: 71–94, 1974.
- Chavrier P, Parton RG, Hauri HP, Simons K, Zerial M. Localization of low molecular weight GTP binding proteins to exocytic and endocytic compartments. *Cell* 62: 317–329, 1990.
- Chen CC, Schweinsberg PJ, Vashist S, Mareiniss DP, Lambie EJ, Grant BD. RAB-10 is required for endocytic recycling in the *Caenorhabditis elegans* intestine. *Mol Biol Cell* 17: 1286–1297, 2006.
- Choe KP, Strange K. Evolutionarily conserved WNK and Ste20 kinases are essential for acute volume recovery and survival after hypertonic shrinkage in *Caenorhabditis elegans*. *Am J Physiol Cell Physiol* 293: C915–C927, 2007.
- Coburn C, Allman E, Mahanti P, Benedetto A, Cabreiro F, Pincus Z, Matthijssens F, Araiz C, Mandel A, Vlachos M, Edwards SA, Fischer G, Davidson A, Pryor RE, Stevens A, Slack FJ, Tavernarakis N, Braeckman BP, Schroeder FC, Nehrke K, Gems D. Anthranilate fluorescence marks a calcium-propagated necrotic wave that promotes organismal death in *C. elegans*. *PLoS Biol* 11: e1001613, 2013.

15. Dal Santo P, Logan M, Chisholm A, Jorgensen E. The inositol triphosphate receptor regulates a 50-second behavioral rhythm in *C. elegans*. *Cell* 98: 757–767, 1999.
16. Di Sole F, Babich V, Moe OW. The calcineurin homologous protein-1 increases Na(+)/H(+)-exchanger 3 trafficking via ezrin phosphorylation. *J Am Soc Nephrol* 20: 1776–1786, 2009.
17. Di Sole F, Cerull R, Babich V, Quinones H, Gisler SM, Biber J, Murer H, Burckhardt G, Helmle-Kolb C, Moe OW. Acute regulation of Na/H exchanger NHE3 by adenosine A(1) receptors is mediated by calcineurin homologous protein. *J Biol Chem* 279: 2962–2974, 2004.
18. Di Sole F, Vadnagara K, Moe OW, Babich V. Calcineurin homologous protein: a multifunctional Ca<sup>2+</sup>-binding protein family. *Am J Physiol Renal Physiol* 303: F165–F179, 2012.
19. Donowitz M, Mohan S, Zhu CX, Chen TE, Lin R, Cha B, Zachos NC, Murtazina R, Sarker R, Li X. NHE3 regulatory complexes. *J Exp Biol* 212: 1638–1646, 2009.
20. Fievet B, Louvard D, Arpin M. ERM proteins in epithelial cell organization and functions. *Biochim Biophys Acta* 1773: 653–660, 2007.
21. Goss G, Orlowski J, Grinstein S. Coimmunoprecipitation of a 24-kDa protein with NHE1, the ubiquitous isoform of the Na<sup>+</sup>/H<sup>+</sup> exchanger. *Am J Physiol Cell Physiol* 270: C1493–C1502, 1996.
22. Gutierrez-Ford C, Levay K, Gomes AV, Perera EM, Som T, Kim YM, Benovic JL, Berkovitz GD, Slepak VZ. Characterization of tescalcin, a novel EF-hand protein with a single Ca<sup>2+</sup>-binding site: metal-binding properties, localization in tissues and cells, and effect on calcineurin. *Biochemistry* 42: 14553–14565, 2003.
23. Jimenez-Vidal M, Srivastava J, Putney LK, Barber DL. Nuclear-localized calcineurin homologous protein CHP1 interacts with upstream binding factor and inhibits ribosomal RNA synthesis. *J Biol Chem* 285: 36260–36266, 2010.
24. Kuwahara H, Kamei J, Nakamura N, Matsumoto M, Inoue H, Kanazawa H. The apoptosis-inducing protein kinase DRAK2 is inhibited in a calcium-dependent manner by the calcium-binding protein CHP. *J Biochem* 134: 245–250, 2003.
25. Lamitina ST, Morrison R, Moeckel GW, Strange K. Adaptation of the nematode *Caenorhabditis elegans* to extreme osmotic stress. *Am J Physiol Cell Physiol* 286: C785–C791, 2004.
26. Li QH, Wang LH, Lin YN, Chang GQ, Li HW, Jin WN, Hu RH, Pang TX. Nuclear accumulation of calcineurin B homologous protein 2 (CHP2) results in enhanced proliferation of tumor cells. *Genes Cells* 16: 416–426, 2011.
27. Li X, Liu Y, Kay CM, Muller-Esterl W, Fliegel L. The Na<sup>+</sup>/H<sup>+</sup> exchanger cytoplasmic tail: structure, function, and interactions with tescalcin. *Biochemistry* 42: 7448–7456, 2003.
28. Lin X, Barber DL. A calcineurin homologous protein inhibits GTPase-stimulated Na-H exchange. *Proc Natl Acad Sci USA* 93: 12631–12636, 1996.
29. Lin X, Sikkink RA, Rusnak F, Barber DL. Inhibition of calcineurin phosphatase activity by a calcineurin B homologous protein. *J Biol Chem* 274: 36125–36131, 1999.
30. Liu Y, Zaun HC, Orlowski J, Ackerman SL. CHP1-mediated NHE1 biosynthetic maturation is required for Purkinje cell axon homeostasis. *J Neurosci* 33: 12656–12669, 2013.
31. Louvet-Vallee S. ERM proteins: from cellular architecture to cell signaling. *Biol Cell* 92: 305–316, 2000.
32. Mailander J, Muller-Esterl W, Dedio J. Human homolog of mouse tescalcin associates with Na(+)/H(+) exchanger type-1. *FEBS Lett* 507: 331–335, 2001.
33. Matsushita M, Sano Y, Yokoyama S, Takai T, Inoue H, Mitsui K, Todo K, Ohmori H, Kanazawa H. Loss of calcineurin homologous protein-1 in chicken B lymphoma DT40 cells destabilizes Na<sup>+</sup>/H<sup>+</sup> exchanger isoform-1 protein. *Am J Physiol Cell Physiol* 293: C246–C254, 2007.
34. Meresse S, Gorvel JP, Chavrier P. The rab7 GTPase resides on a vesicular compartment connected to lysosomes. *J Cell Sci* 108: 3349–3358, 1995.
35. Mishima M, Wakabayashi S, Kojima C. Solution structure of the cytoplasmic region of Na<sup>+</sup>/H<sup>+</sup> exchanger 1 complexed with essential cofactor calcineurin B homologous protein 1. *J Biol Chem* 282: 2741–2751, 2007.
36. Nakamura N, Miyake Y, Matsushita M, Tanaka S, Inoue H, Kanazawa H. KIF1Bbeta2, capable of interacting with CHP, is localized to synaptic vesicles. *J Biochem* 132: 483–491, 2002.
37. Naoe Y, Arita K, Hashimoto H, Kanazawa H, Sato M, Shimizu T. Structural characterization of calcineurin B homologous protein 1. *J Biol Chem* 280: 32372–32378, 2005.
38. Nehrke K. Membrane ion transport in non-excitabile tissues. *WormBook* 1–22, 2014.
39. Nehrke K. A reduction in intestinal cell pH<sub>i</sub> due to loss of the *Caenorhabditis elegans* Na<sup>+</sup>/H<sup>+</sup> exchanger NHX-2 increases life span. *J Biol Chem* 278: 44657–44666, 2003.
40. Nehrke K, Melvin JE. The NHX family of Na<sup>+</sup>-H<sup>+</sup> exchangers in *Caenorhabditis elegans*. *J Biol Chem* 277: 29036–29044, 2002.
41. Nelson FK, Riddle DL. Functional study of the *Caenorhabditis elegans* secretory-excretory system using laser microsurgery. *J Exp Zool* 231: 45–56, 1984.
42. Pang T, Hisamitsu T, Mori H, Shigekawa M, Wakabayashi S. Role of calcineurin B homologous protein in pH regulation by the Na<sup>+</sup>/H<sup>+</sup> exchanger 1: tightly bound Ca<sup>2+</sup> ions as important structural elements. *Biochemistry* 43: 3628–3636, 2004.
43. Pang T, Su X, Wakabayashi S, Shigekawa M. Calcineurin homologous protein as an essential cofactor for Na<sup>+</sup>/H<sup>+</sup> exchangers. *J Biol Chem* 276: 17367–17372, 2001.
44. Pang T, Wakabayashi S, Shigekawa M. Expression of calcineurin B homologous protein 2 protects serum deprivation-induced cell death by serum-independent activation of Na<sup>+</sup>/H<sup>+</sup> exchanger. *J Biol Chem* 277: 43771–43777, 2002.
45. Perera EM, Martin H, Seeherunvong T, Kos L, Hughes IA, Hawkins JR, Berkovitz GD. Tescalcin, a novel gene encoding a putative EF-hand Ca(2+)-binding protein, Col9a3, and renin are expressed in the mouse testis during the early stages of gonadal differentiation. *Endocrinology* 142: 455–463, 2001.
46. Pfeiffer J, Johnson D, Nehrke K. Oscillatory transepithelial H(+) flux regulates a rhythmic behavior in *C. elegans*. *Curr Biol* 18: 297–302, 2008.
47. Sato K, Norris A, Sato M, Grant BDC. *elegans* as a model for membrane traffic. *WormBook* 1–47, 2014.
48. Thwaites DT, Ford D, Glanville M, Simmons NL. H(+)/solute-induced intracellular acidification leads to selective activation of apical Na(+)/H(+) exchange in human intestinal epithelial cells. *J Clin Invest* 104: 629–635, 1999.
49. Thwaites DT, Kennedy DJ, Raldua D, Anderson CM, Mendoza ME, Bladen CL, Simmons NL. H/dipeptide absorption across the human intestinal epithelium is controlled indirectly via a functional Na/H exchanger. *Gastroenterology* 122: 1322–1333, 2002.
50. Vitelli R, Santillo M, Lattero D, Chiariello M, Bifulco M, Bruni CB, Bucci C. Role of the small GTPase Rab7 in the late endocytic pathway. *J Biol Chem* 272: 4391–4397, 1997.
51. Wagner J, Allman E, Taylor A, Ulmschneider K, Kovanda T, Ulmschneider B, Nehrke K, Peters MA. A calcineurin homologous protein is required for sodium-proton exchange events in the *C. elegans* intestine. *Am J Physiol Cell Physiol* 301: C1389–C1403, 2011.
52. Zachos NC, Tse M, Donowitz M. Molecular physiology of intestinal Na<sup>+</sup>/H<sup>+</sup> exchange. *Annu Rev Physiol* 67: 411–443, 2005.
53. Zaun HC, Shrier A, Orlowski J. Calcineurin B homologous protein 3 promotes the biosynthetic maturation, cell surface stability, and optimal transport of the Na<sup>+</sup>/H<sup>+</sup> exchanger NHE1 isoform. *J Biol Chem* 283: 12456–12467, 2008.
54. Zaun HC, Shrier A, Orlowski J. N-myristoylation and Ca<sup>2+</sup> binding of calcineurin B homologous protein CHP3 are required to enhance Na<sup>+</sup>/H<sup>+</sup> exchanger NHE1 half-life and activity at the plasma membrane. *J Biol Chem* 287: 36883–36895, 2012.
55. Zhang-James Y, DasBanerjee T, Sagvolden T, Middleton FA, Faraone SV. SLC9A9 mutations, gene expression, and protein-protein interactions in rat models of attention-deficit/hyperactivity disorder. *Am J Med Genet B Neuropsychiatr Genet* 156B: 835–843, 2011.